



## ORIGINAL RESEARCH

# Method for optimising the performance of PML in anchor-loss limited model via COMSOL

Peng Li<sup>1</sup>  | Jun-Yu Ou<sup>2</sup>  | Jize Yan<sup>1</sup><sup>1</sup>Electronics and Computer Science, University of Southampton, Southampton, UK<sup>2</sup>Optoelectronics Research Centre, University of Southampton, Southampton, UK**Correspondence**Jize Yan, Electronics and Computer Science,  
University of Southampton, Southampton, United  
Kingdom.

Email: J.Yan@soton.ac.uk

**Funding information**Engineering and Physical Sciences Research Council,  
Grant/Award Number: EPSRC EP/V000624/1**Abstract**

Perfectly matched layer has been used for solving anchor-loss limited quality factor in the Micro electromechanical systems. However, setting up a well-behaved perfectly matched layer requires users to change the parameters of a perfectly matched layer to give correct results, while the current existing methods for choosing the right parameters are vague and lack theoretical support. Based on the mathematical theory of perfectly matched layer and simulation results of a beam structure's quality factor, this paper proposes a method for choosing the parameter to optimise the performance of perfectly matched layer in COMSOL. The accuracy of the proposed method is proved by matching the effect of substrate height on beam's quality factor with theory prediction. The author also studies the effect of beam height and beam width on the quality factor of the beam. The results demonstrate that simulated quality factors are in agreement with analytical values when the ratio of height over length is small but will show great divergence when height equals the length. This trend can be observed for the beam width as well. Especially for larger ratio of beam width over beam length, instead of decreasing monotonously as analytical equation would expect, the simulated quality factor will converge into a stable value of 1700, which matches the result of two-dimensional model for the same beam structure. This means that a three-dimensional model has to be used for estimating the quality factor of a beam structure.

## 1 | INTRODUCTION

Micro-electromechanical systems (MEMS) have many applications and the control of energy loss has been one of the main issues during the design for MEMS [1]. The measurement parameter for the energy loss is the quality factor (Q factor) [2]. Depending on scale, geometry and material, the energy loss may come from material damping, air damping, thermoelastic damping or the radiation of elastic wave from an anchor (aka anchor loss) [2–7]. Among them, anchor loss is believed to be the main loss in high-frequency resonators [7].

In most designs, the resonating device is much smaller than the substrate it sits on and the bulk of the chip can be modelled as a semi-infinite half-space [8]. But in practice, most MEMS problems are solved via finite element method (FEM) or finite difference method (FDM). In order to simulate the design via FEM or FMD, a finite domain is required [9]. So in order to

simulate the design as a semi-infinite space, adding an artificial absorbing boundary at a finite domain is essential [9]. There are many different absorbing boundary conditions, such as boundary dampers, infinite elements, boundary integrals, Dirichlet-to-Neumann (DtN) boundary conditions, and perfectly matched layer (PML) [8–15].

Among all the conditions, PML has the advantages of being easily implemented into FEM, economically low cost for computer power, and theoretically absorbing waves from any angle of incidence [14, 15]. And many researchers have been using PML installed in COMSOL for their own designs [16–24].

However, when PML is implemented within FEM (as shown in Figure 1), there are reflections from the end of the PML or the interface between PML and bounded domain [15]. Such reflections are related with a parameter defined as PML scaling parameter  $\beta$  [15]. So in order to optimise the performance of the PML, users need to choose proper parameters [16, 20].

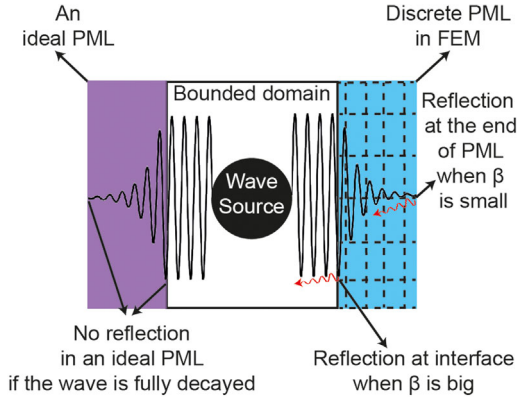


**FIGURE 1** Schematic of the waves decayed in an ideal PML and in a discrete PML. In both situations, the wave will be attenuated and an addition of the PML will not affect the wave propagating inside the bounded domain. In an ideal PML, there will be no reflection at all. However, when PML is discretised within FEM, there will be reflections from the end of PML or the interface between PML and bounded domain. Such reflections depend on the value of a parameter defined as PML scaling parameter  $\beta$  [15]

However, the accurate method for setting up the parameters for using PML in COMSOL is not well studied.

Currently, there are two different widely accepted methods. The first method is proposed by *Vikram* and *Mina* [16]. They claimed that by sweeping a parameter defined as PML scale factor  $\alpha$  in COMSOL, one could find the minimum value of Q factor. If the minimum Q factors could match with the analytical estimates of Q factors for beams with various sizes, the corresponding parameters should be chosen for their own models [16]. This method has been adopted by some other researchers [17–19]. It can be seen that the accuracy of the analytical results is vital in this method. The analytical equation that *Vikram* and *Mina* used in [16] is a 2D model proposed by *Hao* [25], which in the following section the author will show that this analytical equation is not accurate.

The second method is suggested by *Ali Darvishian et al.* [20]. They suggested that  $\alpha$  should be kept as 1. Their simulations results showed that in the range between 0.2 and 2, the simulated Q factors are almost the same [20]. This method is based on their understanding and discussion with experts at COMSOL [20] and it has also been accepted by some researchers [21–24]. Although this method seems to be correct, the choice of  $\alpha$  and the range is vague. There is also a lack of theoretical support for these decisions. These two methods provide different ways to find the optimised parameters for the PML, which is confusing for researchers who need to use PML via COMSOL.

Author will first present the definition of  $\beta$  based on the theory from [15] and  $\alpha$  from COMSOL manual [26]. Then the link and the difference of  $\alpha$  and  $\beta$  will be analysed by making comparison between the different definition equations of PML from [15] and [26]. The theory about how  $\beta$  affects the performance of the PML [15, 27] will also be presented here. In this way, we can predict how the change of  $\alpha$  will affect the performance of PML. Afterwards, the author will combine the theory with a simulation result of a beam structure, and a

new method to optimise the performance of PML in COMSOL will be proposed. The accuracy of the method is then validated by matching the simulation results of the effects of substrate height on beam's Q factor with theory prediction. Finally the author studies the impacts of beam width and beam height on beam's Q factor, showing that the current analytical equation is only reliable when beam length is much bigger compared to beam width and beam height. And a 3D model has to be used for simulating the Q factor correctly for a beam structure.

## 2 | THE LINK AND THE DIFFERENCE BETWEEN $\alpha$ AND $\beta$

### 2.1 | The definition of $\alpha$ and $\beta$

To be able to find the link and the difference between  $\alpha$  and  $\beta$ , it is necessary to understand the theory of PML and how the parameter is defined, especially the definition of  $\alpha$  and  $\beta$ .

It is worth mentioning that PML can be either interpreted as a coordinate stretching [15, 28] or a complex-valued change of material properties [15, 29]. Here, the author will focus on the understanding of coordinate stretching [15, 28].

Let us focus on a 1D elastic wave, consider a longitudinal wave propagating in a homogeneous, semi-infinite rod with axial coordinate  $x \in (0, \infty)$ . Also, the wave travels at the speed  $c$ , then the wave equation that describes this system is

$$\frac{\partial^2 u}{\partial x^2} - \frac{1}{c^2} \frac{\partial^2 u}{\partial t^2} = 0, \quad (1)$$

where  $u(x, t)$  is the displacement.  $u(x, t)$  is a time harmonic function that can be described as  $u(x, t) = \hat{u}(x)e^{i\omega t}$ , and its amplitude  $\hat{u}(x)$  is governed by a Helmholtz equation:

$$\frac{d^2 \hat{u}}{dx^2} + k^2 \hat{u} = 0, \quad (2)$$

where  $k = \omega/c$  is the wave number, and solution to the Helmholtz equation is

$$\hat{u} = c_{\text{out}} e^{-ikx} + c_{\text{in}} e^{ikx} \quad (3)$$

where  $c_{\text{out}}$  is the magnitude of the outgoing wave travelling from the origin towards infinity, and  $c_{\text{in}}$  is the magnitude of the incoming wave travelling from infinity towards the origin.

Now we can consider the Helmholtz equation under a change of coordinate. Define a continuous function  $\lambda(s)$ , which is nowhere zero, and a new coordinate  $x^*$

$$x^* = \int_0^x \lambda(s) ds \quad \text{with} \quad \lambda(s) = 1 - i\sigma(s)/k, \quad (4)$$

$\lambda(s)$  is defined as stretching function, and it is related with attenuation function  $\sigma(s)$  [15]. As it is shown in Figure 2, let

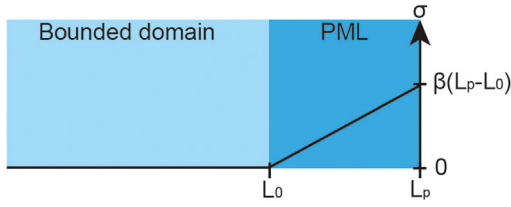


**FIGURE 2** Illustration of piecewise linear attenuation function  $\sigma(s)$ : in the bounded domain  $\sigma(s) = 0$  while inside the PML  $\sigma(s)$  increases linearly with the coordinate.  $L_0$  and  $L_p$  are the coordinate where the PML starts and ends, separately. The linear slope  $\beta$  is defined as PML scaling parameter. And the value of  $\beta$  would decide the attenuate rate and how far the coordinate would stretch inside the PML [15]

us assume  $\sigma(s)=0$  inside the bounded area when  $x \in (0, L]$ , while  $\sigma(s) = \beta(s - L)$  when  $x \in [L, \infty)$ . Then for  $x > L$ , the stretched coordination  $x^*$  can be expressed as

$$x^* = L + \int_L^x \lambda(s) ds = x - i \frac{\beta(x - L)^2}{2k} \quad (5)$$

the outgoing wave amplitude and incoming wave amplitude will become  $c_{out} \exp(-\beta(x - L)^2/2)$  and  $c_{in} \exp(\beta(x - L)^2/2)$ , separately. It can be seen that during the region where  $\sigma(s) = 0$ , there will be no change to the coordinate and the wave solution. But in the PML region where  $\sigma(s) > 0$ , the outgoing wave amplitude will decay with increasing  $x$  and the incoming wave amplitude will decay with decreasing  $x$  [15].

Here  $\beta$  is defined as PML scaling parameter [15], based on the fact that this parameter defines how far the coordinate would be stretched or scaled over the PML, and it can also be seen that it will decide how fast the wave would decay inside the PML [15]. The bigger the  $\beta$ , the faster the wave will be attenuated, and the further the coordinate will be stretched [15]. And this is what we expect a PML to behave even we solve the problem in the finite domain [15].

PML in the COMSOL follows the same philosophy, changing real coordination into complex one [26]. However, compared with Equation (5), the PML in COMSOL has adopted a different equation for coordinate stretching, which can be found from COMSOL manual reference [26].

$$x^* = x_0 + \left( \frac{x - x_0}{\Delta\omega} \right)^n (1 - i)\lambda\alpha. \quad (6)$$

Where  $x_0$  is the coordinate at the beginning of PML,  $\Delta\omega$  is the thickness of PML,  $n$  is defined as curvature scale factor and normally set as 1,  $\lambda$  is the typical wavelength. And for eigen-frequency study, as the frequency is unknown, therefore the wavelength  $\lambda$  is unknown. In COMSOL setting, this parameter will be automatically replace by PML thickness  $\Delta\omega$  [26].

Among all these parameters,  $\alpha$ , which is defined as the PML scale factor, is the key parameter that users need to properly set up to optimise the accuracy of PML, and the one that current two method have disagreement on [16, 20].

## 2.2 | The link and the difference between $\alpha$ and $\beta$

After knowing the definition of  $\alpha$  and  $\beta$ , now we can analyse the link and the difference between these two parameters. Comparing Equation (6) with Equation (5), it can be seen that in terms of the imaginary part of the coordinate, once all the other parameter decided, both  $\alpha$  and  $\beta$  will have linear function with the change of the imaginary part of the coordinate.

From the previous part, we know that  $\beta$  will control how fast the wave will be attenuated and how further the coordinate will be stretched inside PML. When  $\beta$  is small, the wave inside the PML will not be attenuated quick enough before it reaches the end of the PML, and there will be reflection from the end of PML. Conversely, when  $\beta$  is too big, the mesh density mismatch at the interface between PML and bounded domain will increase due to big stretch in the coordinate. This mismatch will lead to an increased reflection [15].

Similar effect of  $\beta$  is also reported in [27]. As  $\alpha$  has the same linear function as  $\beta$  in deciding attenuation rate and coordinate stretching, it can be deduced that the change of  $\alpha$  will also lead to different numerical reflections and there will be an optimised value for  $\alpha$ . This is why *Vikram* and *Mina* suggested to sweep  $\alpha$ , so that they could find the optimised value for  $\alpha$  [16].

However, from Equation (6), it can be seen that  $\alpha$  will also modulate the real part of the coordinate. Such setting could be useful for some other problems [30], but a modulation in the real part will alter the frequency slightly and Q factor calculated as  $|Re(\omega)/2Im(\omega)|$  is sensitive to the change of the frequency [31], where  $Re(\omega)$  and  $Im(\omega)$  are the real and imaginary parts of the angular resonator frequency  $\omega$  of the mode.

Due to this difference between  $\alpha$  and  $\beta$ , there will be more restrictions for choosing the proper  $\alpha$  to optimise the performance of the PML. In the following subsection, the author will combine this theory with the simulation results of a beam structure. Based on the simulation results, a new method for optimising the performance of PML via COMSOL will be proposed.

## 3 | THE METHOD FOR OPTIMISING THE PERFORMANCE OF PML

To find out the influence of  $\alpha$  on the Q factor, the author studies the Q factor of the fundamental out-of-plane mode in a beam resonator as shown in Figure 3. The simulation setting is illustrated in Figure 3(a), the beam is described by length  $L$ , height  $H$ , and width  $W$ . The beam is sitting on a sphere substrate with radius of  $W_{sub}$ . A PML of  $T_{PML}$  thickness is attached to the substrate in all direction. By doing so, a finite domain will be effectively equal to an infinite domain [15]. A symmetry plan is applied in  $x - y$  plane to reduce the simulation time and power. Figure 3(b) shows the normalised total displacement of the fundamental out-of-plane mode.

To obtain the numerical result, the author randomly chooses the size of the beam to be  $L=10 \mu\text{m}$ ,  $H=1 \mu\text{m}$ ,  $W=1 \mu\text{m}$ .

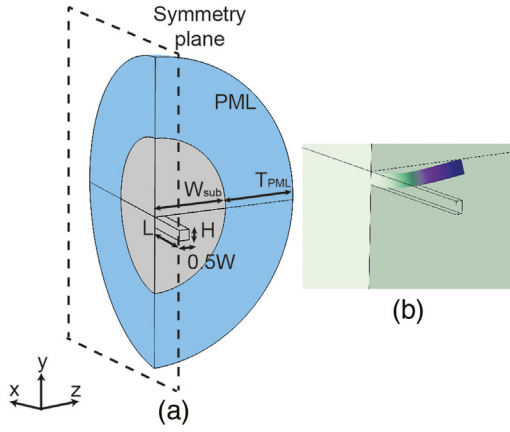


**FIGURE 3** Illustration of the 3D model for the study of Q factor of the fundamental out-of-plane mode of a clamped-free beam. The beam is described by length  $L$ , height  $H$ , and width  $W$ . And the beam is sitting on a sphere substrate with radius of  $W_{\text{sub}}$ . A PML of  $T_{\text{PML}}$  thickness is attached to the substrate. A symmetry plan is applied in  $x-y$  plane to reduce the simulation time and power. (a) Schematic of the model used for the study of Q factor of the fundamental out-of-plane mode of a clamped-free beam. (b) Normalised total displacement of the fundamental out-of-plane mode

The material of the beam and substrate is chosen to be silicon, with density  $\rho$ , Young's modulus  $E$  and Poisson's ratio  $\nu$  to be 2230 kg/m<sup>3</sup>, 130 GPa and 0.3, respectively. For a beam with rectangular cross-section, its first bending eigenfrequency  $\omega_0$  could be estimated by Euler-Bernoulli theory [32],  $\omega_0 = (1.875/L)^2 \sqrt{EH^2/(12\rho)}$ , which is 12.07 MHz for our studied beam. As for calculating the Q factor of this mode, there are few different analytical equations. The author summarises these equations in the following subsection.

### 3.1 | Analytical equations for calculating the Q factor of the beam

The first analytical equation for the Q factor of the fundamental out-of-plane mode of a clamped-free beam is provided by *Jimbo* and *Itao* [33]. It treated the vibration of a beam as an elastic wave and the support loss was not derived from the viewpoint of the resonant modes of a beam resonator, hence the expression is only closed form [33].

$$Q \approx 2.1654 \frac{L^3}{H^3} \frac{E_b}{E}, \quad (7)$$

where  $E_b$  and  $E$  denote the Young modulus of the beam and substrate, respectively.

Afterwards, *Hao* derived a more accurate analytical equation based on above analytical equation [25]:

$$Q = \left[ \frac{0.24(1-\nu)}{(1+\nu)\Psi} \right] \frac{1}{(\beta_n \chi_n)^2} \left[ \frac{L}{H} \right]^3, \quad (8)$$

where  $\nu$  is the Poisson's ratio,  $\Psi$  is a coefficient related with mode displacement,  $\beta$  and  $\chi$  are mode constant and mode

**TABLE 1** Analytical values of different equations for a same beam

Reference resource	Estimate results	2D or 3D
Jimbo [33]	2165.4	2D
Hao [20]	2081	2D
Judge [21]	323,000	3D

shape factor, respectively [25]. This analytical equation has been used to calculate the target value for choosing the best  $\alpha$  by *Vikram* and *Mina* [16].

Recently, many researchers have reported that the substrate height could heavily effected the Q factor of the beam structures [34–36]. *Photiadis* has showed that a resonator attached to a thick substrate can achieve several time higher Q factor than a resonator attached to a substrate with the same thickness as the resonator or a semi-infinite substrate [34]. Afterwards, an estimate equation for the Q factor is given by *Judge* when the substrate height is semi-infinite [35]. And *Frangi* has obtained a simulation result matching with this equation in a custom Fortran code [28]:

$$Q \approx C \frac{L}{W} \left( \frac{L}{H} \right)^4, \quad (9)$$

where  $C$  is a constant depending on the Poisson coefficient, with  $C = 3.45$  for  $\nu = 0.25$ ,  $C = 3.23$  for  $\nu = 0.3$ ,  $C = 3.175$  for  $\nu = 1/3$  [35]. Here the model will take  $C = 3.23$  as  $\nu = 0.3$ .

In Table 1, the author summarises the analytical values for the beam structure studied in this paper. It can be seen Equations (7) and (8) are only related with beam length  $L$  and beam height  $H$ , which is a 2D model. Equation (9) includes the information of beam size in all directions, which is a 3D model. In the following sections, the author will use a 3D model to study the method to optimise the performance of PML, and show that both Equations (7) and (8) are not accurate to estimate the Q factor for 2D model at the end of this paper.

### 3.2 | The method for optimising the performance of PML

The author studies the Q factor of the beam as illustrated in Figure 3(a). To begin with, the author follows the geometry design and meshing setting suggested in [20]. The substrate width is set to be  $\lambda$  and PML is set to be  $2\lambda$ . In this way, the PML is placed enough far away from the origin of the vibration and PML is thick enough to fully absorb the propagation wave [20]. The distribution meshing is used for PML, and the amount of meshing node is 30. The beam and substrate is meshed with free tetrahedral and the quality is extremely fine defined via COMSOL.

Then  $\alpha$  is swept. The full spectrum of Q factor and frequency as a function of the  $\alpha$  is shown in Figure 4(a). It can be seen that the change of  $\alpha$  would affect eigenfrequency  $\omega_0$ , and a tiny variation in the frequency can induce significant change in the Q



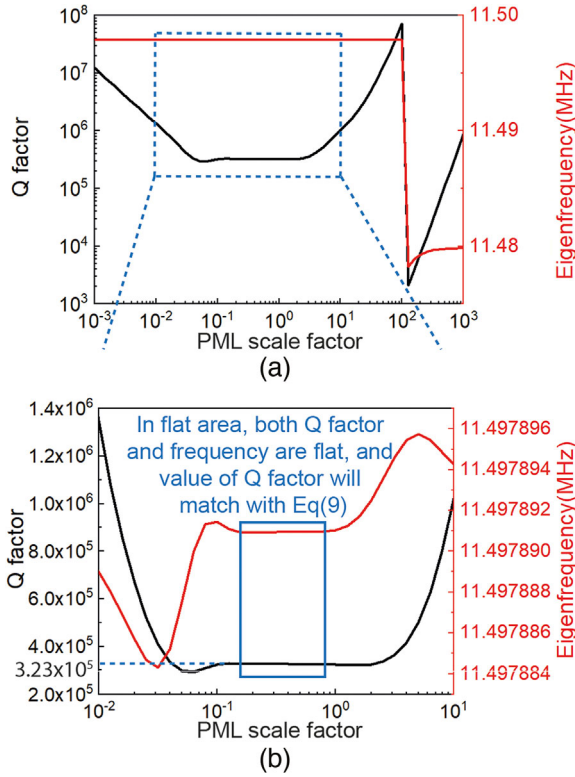


**FIGURE 4** Q factor (black line) and eigenfrequency (red line) as a function of PML scale factor  $\alpha$ : (a) The full spectrum. As the  $\alpha$  is swept, it can be seen that when  $\alpha$  is above 100, there will be a change of 0.1 MHz in the frequency, leading to  $10^5$  change in the Q factor, confirming that a small deviation in the frequency will affect the Q factor largely [31], and there will be a bottom valley at the value of Q factor. (b) The zoomed spectrum of this valley. And there is a range where eigenfrequency and Q factor are both flat and stable. The Q factor within this range will match with the analytical value of Equation (9). The suggested sweep range from [20] covers this region. (a) Full spectrum of Q factor (black line) and frequency (red line) as  $\alpha$  is scanned from  $10^{-3}$  to  $10^3$  (b) Zoomed area from  $\alpha = 10^{-2}$  to  $10^1$ , where Q factor is at the bottom valleys of its values

factor (when  $\alpha$  is bigger than 100). This slight variation in  $\omega_0$  is due to the  $\alpha$ 's modulation of the real part of the coordinate [31]. Although such a modulation of the real part of the coordinate could have advantages in certain problems [30], it will alter the frequency slightly and thus affect the Q factor which is sensitive to the change of  $\omega_0$  [31]. The modulation of the real part of the coordinate displacement is shown Figure 5. It can be seen that different values of  $\alpha$  would stretch the real part of the coordinate differently. And only when  $\alpha$  is equal to 1, the real part of the coordinate will not be changed.

In Figure 4(a), it can also be seen that there is a region where the Q factor is at the bottom valley. Figure 4(b) shows the zoomed-in details in this valley. There is a region where both Q factor and the frequency are flat, and the Q factor within this range matches with the analytical value of Equation (9). And the suggested sweep range from [20] is from 0.2 to 2, which covers this range. However, in the following section, the author will show that the flat range is not fixed and closely related with PML thickness.

We also simulate the same beam in the 2D model in the COMSOL (see [Supplementary Information](#)), and the same flat region can also be found and the simulated Q factor of 1660 is obtained within the region. This simulated result is about 20% smaller compared to the analytical value of Equations (7) and (8). In Section 5, we will show that our simulation results are more reliable. And the inaccuracy of the analytical values could be due to the fact that the coupling effect between the normal stress and shear stress [37] and the influence of Casimir force [38] are not considered in [25].

To summarise, a new method for optimising the performance of PML in COMSOL is proposed: with all the geometry size fixed, especially PML thickness, one could sweep the value of  $\alpha$  in PML, and find the region the Q factor value is at the bottom valley. And the optimised value of  $\alpha$  should be chosen from the region where both Q factor and frequency are flat inside this bottom valley.

### 3.2.1 | Relation of PML thickness and the sweep range of $\alpha$

In [20],  $\alpha$  is suggested to be swept from 0.2 to 2. However, the sweep range of  $\alpha$  is not fixed. The author found out that it is directly related with the PML thickness based on the simulation results. Table 2 summarises the values of  $\alpha$  and Q factor within the flat range for different PML thickness. It shows that the values of  $\alpha$  will become bigger with the decrease in the thickness of the PML layer. And this is due to the fact that the attenuation rate has to increase to compensate the reduction in the PML thickness. The increase of  $\alpha$  will enhance the attenuation rate inside the PML.

And we also note that if the PML layer is too thin, the Q factor will be higher than the expected value. This is due to the failure to fully absorb the wave when PML is too thin. This phenomenon has been reported by Frangi [28], and they gave an empirical rule for choosing PML thickness of  $W_{PML} > \lambda/10$  in their custom Fortran code [28]. Our simulation results indicate a slightly wider range of  $W_{PML} > \lambda/14$ .

To summarise, the PML thickness could be varied within a certain range ( $\lambda/14 < W_{PML} < 2\lambda$ ). For different  $W_{PML}$ , there will be an optimised value of  $\alpha$ . The thinner the  $W_{PML}$  is, the bigger the optimised value of  $\alpha$ . With bigger  $W_{PML}$ , the

**TABLE 2** The range of  $\alpha$  and corresponding Q factor within the stable range of different PML thickness

PML thickness ( $\mu\text{m}$ )	Stable range of $\alpha$	Q factor within the range ( $\times 10^5$ )
10	10–14.12	4.378–4.476
30	6.3–8.9	3.422–3.518
50	3.5–5	3.229–3.231
100	1.77–2.51	3.229–3.231
300	0.7–1.2	3.229–3.231
600	0.18–0.79	3.229–3.231

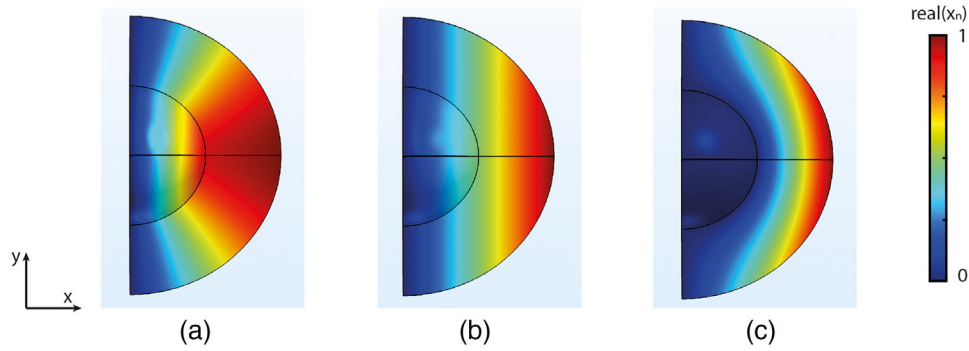


**FIGURE 5** Normalised real part of the coordinate displacement  $real(x_n)$  in  $x$  direction with different  $\alpha$  from the model shown in Figure 3: it can be seen that the change of  $\alpha$  will modulate the real part of the coordinate, resulting in a slight change of the frequency and such a small variation could lead to big change in the Q factor [31]. (a) Normalised real part of the coordinate displacement  $real(x_n)$  when  $\alpha = 10^{-3}$  (b) Normalised real part of the coordinate displacement  $real(x_n)$  when  $\alpha = 1$ . (c) Normalised real part of the coordinate displacement  $real(x_n)$  when  $\alpha = 10^3$

computational complexity will also increase due to the increase of simulation area and meshing node points.

In the following section, the author will apply this method to study the effect of substrate height on the Q factor of the beam structure.

#### 4 | THE IMPACT OF SUBSTRATE HEIGHT ON THE BEAM'S Q FACTOR

The impact of substrate height on the beam's Q factor has been reported by different researchers [34–36]. And Photiadis has showed that a resonator attached to a thick substrate can achieve several time higher Q factor than a resonator attached to a substrate with the same thickness as the resonator or a semi-infinite substrate [34]. Here the author uses a thin plate model (as shown in Figure 6(a)) to analyse the impact of substrate height on Q factor of the beam.

The PML is added in the radial direction to make sure all the waves propagating in radial direction is well and fully absorbed. From previous study, a PML with  $50 \mu\text{m}$  thick is used in this model, which will be enough to fully absorb the propagating wave. And we applied our proposed method to find the optimised  $\alpha$  for the best performance of the PML (as it is shown in Figure 6(b) and (c), and a value of 3.98 for  $\alpha$  is fixed here.)

Figure 6(d) shows the Q factor as a function of substrate width in the radial direction after the PML is properly set up. The result shows that when PML is placed far away enough from the origin of the vibration, the Q factor will become stable. And a thickness of  $50 \mu\text{m}$  of substrate is used for our model.

Then the substrate height  $H_b$  is scanned, and Figure 6(e) shows how the Q factor evolves with  $H_b$ . And the results are in good agreement with the theoretical predictions from [34]. Here some key points are marked in the Figure 6(e). The first marked point is  $360 \mu\text{m}$ , where when the substrate height is below this value, the Q factor is predicted to increase quadratically with the substrate height [34] (details fitting see in the [Supplementary](#)). And then the Q factor would reach a maximum value at  $460 \mu\text{m}$ , which is much higher compared to the value when substrate is

semi-infinite [34]. And when substrate height is beyond  $920 \mu\text{m}$ , the Q factor will converge to a stable value and its value is the same value that we get from the previous model illustrated in Figure 3(a), which confirms the fact that one could apply PML to a finite domain to mimic an infinite space [15].

So up to this stage, the accuracy of the our proposed method has been validated. In the following section, the author will investigate the effect of beam width and beam height on the Q factor with the new method. And the results reveal that: first the current analytical equations are only valid when beam length is much bigger compared to beam width and beam height; second a 3D model containing the size information of the beam in all directions as well as the substrate height has to be used for obtaining the correct Q factor of a beam structure.

#### 5 | THE EFFECT OF BEAM HEIGHT AND BEAM WIDTH ON Q FACTOR

##### 5.1 | Effect of beam height on Q factor

The beam height  $H$  is swept in the same model as we use in Section 3, and the  $\alpha$  is optimised based on our proposed method. During the sweep, all the parameter for the PML will be fixed. Only the substrate width will increase in the direction of beam height, so that the PML is guaranteed to be far away enough from the origin of the vibration. And the results are shown in Figure 7. It can be seen from Figure 7(a) that the simulated frequency will shift further away from the predicted values by Euler–Bernoulli theory [32] with increasing  $H$ . Figure 7(b) also indicates the mismatch between simulated Q factor and analytical values of Equation (9) is getting bigger with the increase of  $H$ . It will eventually reach up to a 200% mismatch when beam height equals to the beam length. The results show that Equation (9) is only valid when the beam structure could be well described by Euler–Bernoulli theory. And when the aspect ratio of height to length is close to 1.0, the structure no longer constitutes a resonator, and it is hard to be excited to vibrate.

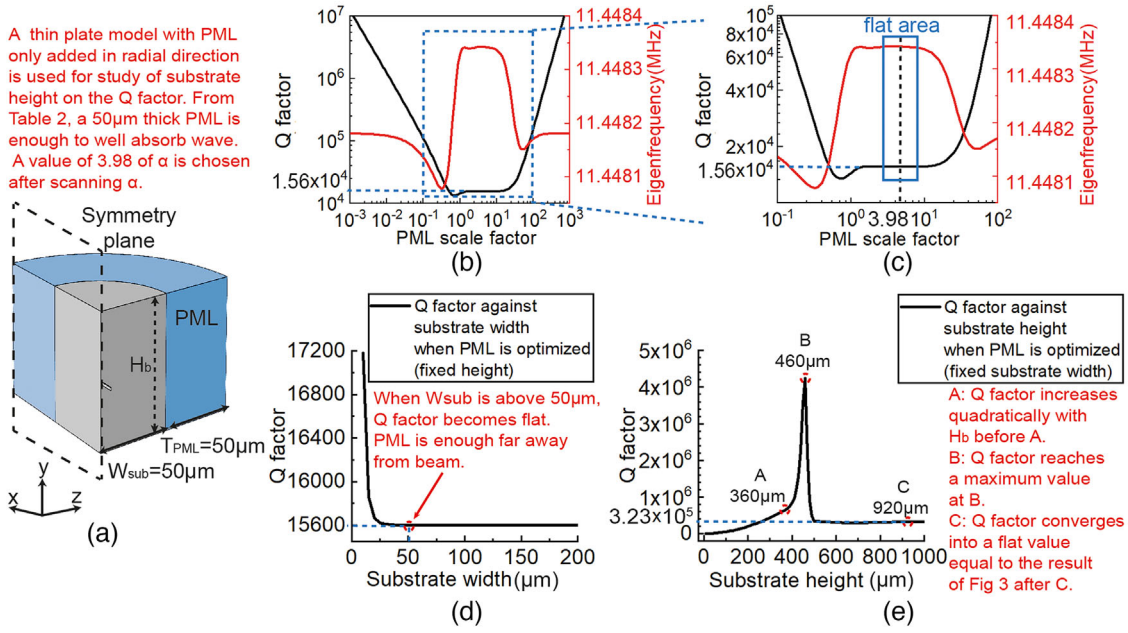


**FIGURE 6** The simulation results of the effect of the substrate height on the Q factor of the beam resonator. A PML is added in the radial direction to make sure that all the waves propagated in the radial direction is well absorbed. The Q factor and eigenfrequency as a function of  $\alpha$  is illustrated in (b) and (c). A proper  $\alpha$  of 3.98 is fixed for the best performance of the PML based on our method. A sweep of substrate width is conducted after  $\alpha$  is fixed and the results is shown in (d). It can be seen that after 50  $\mu\text{m}$ , the Q factor is stable. Therefore, a value of 50  $\mu\text{m}$  is used to make sure the PML is far away enough and will not affect the Q factor. And (e) shows how the Q factor will evolve with the increasing  $H_b$ . The Q factor would first increase quadratically with the substrate height until 360  $\mu\text{m}$  and then reach a maximum value at 460  $\mu\text{m}$  which is well excess of the stable value predicted by Equation (9) of 323,000 after  $H_b$  over 920  $\mu\text{m}$ . (a) The schematic of the model used for the study of substrate height's impact on the Q factor of the beam resonator. (b) Full spectrum of Q factor (black line) and frequency (red line) as  $\alpha$  is scanned from  $10^{-3}$  to  $10^3$  for the model illustrated in (a) (c) Zoomed spectrum around the stable region for (a), and a value of 3.98 is chosen for the optimisation of the PML. d) Q factor as a function of substrate width when  $\alpha$  is set at 3.98. e) Q factor as a function of substrate height  $H_b$ .

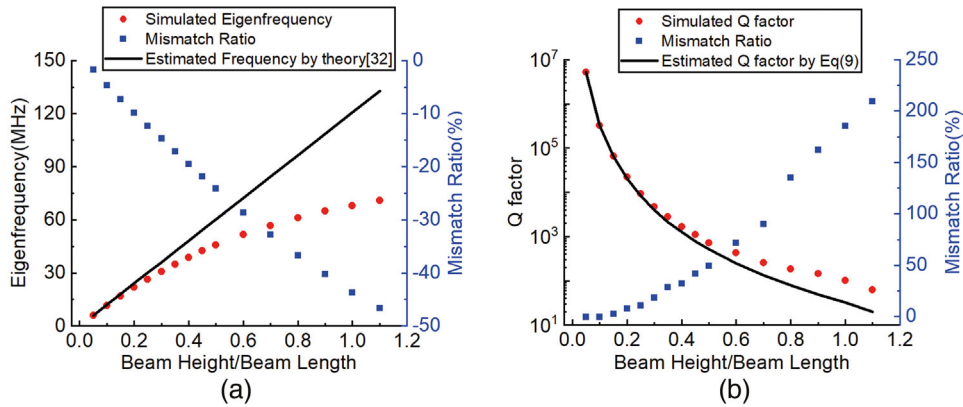


**FIGURE 7** The results of beam height's effect on the frequency and the Q factor. (a) The frequency as a function of the ratio of beam height over beam length. It can be seen that with the increasing of the beam height, the simulated frequency will shift further and further away from the estimated values of Euler–Bernoulli theory [32]. And combined with (b), shows the Q factor as a function of the ratio of beam height over beam length. It can be seen that when the beam can no longer be described by the Euler–Bernoulli theory, the simulated results will start to diverge from the analytical values and reach more than 200% mismatch when beam height equals the beam length. (a) Frequency as a function of the ratio of beam height over beam length. (b) Q factor as a function of the ratio of beam height over beam length.

## 5.2 | Effect of beam width on Q factor

The beam width  $W$  is also swept. And all the geometry design and meshing setting are the same with the study of beam height. The results are summarised in Figure 8. Unlike the beam

height, the change of beam width is not expected to change the frequency of the fundamental mode. However, our simulated results shows that the frequency will increase slightly from 11.498 MHz to 11.82 MHz, but overall it is still within the estimated value of Euler–Bernoulli theory [32].

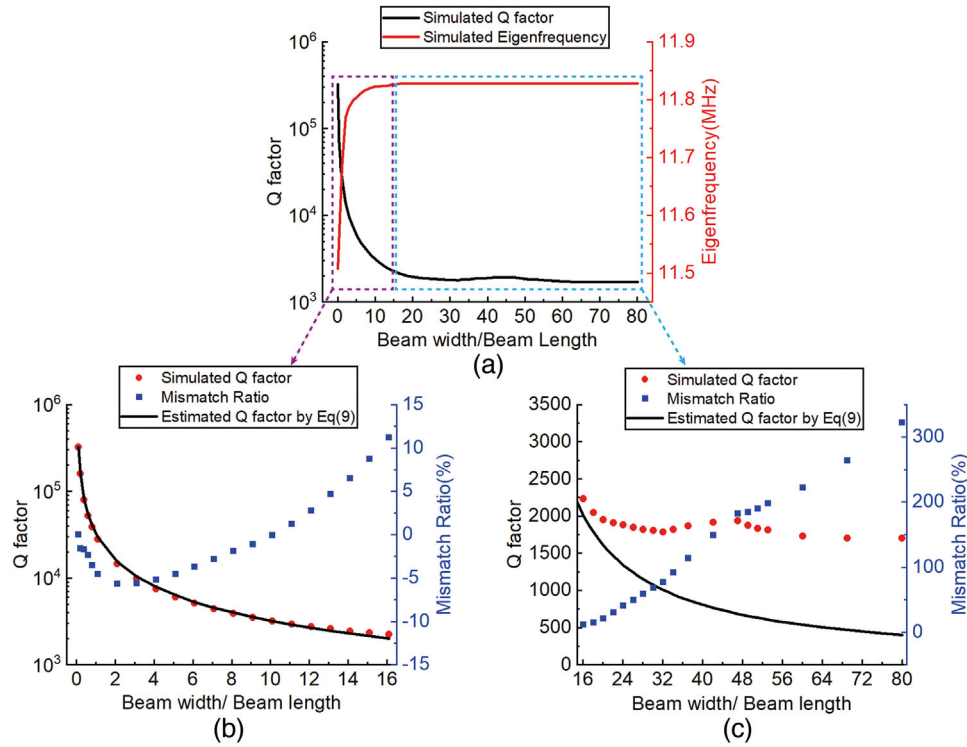


**FIGURE 8** The results of beam width's effect on the frequency and the Q factor. (a) The frequency and the Q factor as a function of the ratio of beam width over beam length. It can be seen that with the increase of the beam width, the frequency will slightly increase from 11.498 MHz to 11.82 MHz and the Q factor will become stable when beam width is large. (b) and (c) The details of the evolution of Q factor with beam width increasing. From (b) it can be seen that when the ratio is below 16, the simulated results fit well with analytical values with maximum 10% mismatch ratio, indicating that the analytical equation is valid in this region. However, with beam width continuing to grow, the simulated results show divergence with analytical values. Especially when the beam width is large, the Q factor will converge into a stable value of 1700, instead of decreasing monotonously predicted by Equation (9). (a) Frequency and Q factor as a function of the ratio of beam width over beam length. (b) Zoomed details of Q factor when the ratio is below 16. (c) Zoomed details of Q factor when the ratio is above 16

On the other hand, the Q factor shows a different evolution compared to the theoretical prediction of Equation (9). Figure 8(b) and (c) shows the zoomed details of the change of Q factor against the ratio of beam width over beam length. In Figure 8(b), it can be seen that in the region where the ratio is within 16, the simulated Q factor could be well estimated by Equation (9), with up to only 10% mismatch ratio.

However, when the beam width continues to grow, the simulated results will diverge from the analytical values. It can be seen in Figure 8(c), the predicted Q factor will decrease monotonously as the width increases. However, the simulated results show that the Q factor will undergo a slight increase first and then converge into a stable value of 1700.

The reason for the small bump could be the same reason for the peak in the Q factor as the substrate height  $H_b$  changes, which is due to the match between the wavelength and the beam width. The resonance is formed in the width direction and leading to the increasing of the Q factor [34].

And it also brings to our attention that the converged Q factor in the 3D model matches with the simulated results of our 2D model. This can be explained by the plane strain theory in solid mechanics [39]. When the beam width is much bigger, both plane strain problem and plane stress

**TABLE 3** Comparison between 2D analytical values, 2D model and 3D model when the beam width is large

Refereed resource	Jimbo [33]	Hao [20]	3D model (beam width is large)	2D model
Eigenfrequency (MHz)	12.07	12.07	11.82	11.83
Q factor	2165.4	2081	1700	1660

problem belong to plane problem, and can be treated in unified approach [39].

This finding proves that our simulation results from the 2D model is accurate. From previous sections, we know that analytical values of Equations (7) and (8) are around 20% bigger than simulated results of the 2D model. It is believed that the reason for the inaccuracy in the analytical equations is coming from the restrictive decoupling assumption employed in the analytical derivation [24]. Table 3 summarises the results of analytical values of the 2D equations, the 2D model and the 3D model when Q factor is converged. Beams with different sizes are also simulated and the simulations results show the same conclusion (see in Supplementary).



## 6 | CONCLUSION

The authors propose a new method to optimise the performance of the PML for the analysis of anchor-loss limited Q factor in COMSOL. The value of a parameter defined as PML scale factor  $\alpha$  is proved to be crucial for the accuracy of simulation results. The proper choice of  $\alpha$  will lead to the stability of both Q factor and eigenfrequency. Also, the accuracy of the method is validated by matching the simulation results of substrate height's impact on Q factor with the theory prediction.

The effects of beam height and beam width on the Q factor of the beam are also studied based on the proposed method. It shows that the current analytical equation for calculating the Q factor of the beam is only reliable when the beam could be well described by Euler–Bernoulli theory and when beam width is small.

Especially when the beam width is much bigger, our simulation shows that both the frequency and the Q factor of the 3D model will move closer to the results of the 2D model for the same beam. On one hand, this proves the accuracy of the 2D simulation results. On the other hand, it also shows that in 2D the widely accepted analytical equations will lead to errors up to 20% due to restrictive decoupling assumption. This means that a 3D model containing the substrate height and the beam sizes in all direction is crucial for obtaining the accurate Q factor for the beam structure. The robustness of this method will help to improve the accuracy in the prediction of the Q factor dominated by anchor dissipation in other MEMS resonators designs.

## ACKNOWLEDGEMENTS

The author would like to acknowledge Mr Shengqi Yin for the valuable opinions during the writing of this paper and Mr Chuang Sun for the helpful discussion about mechanical engineering. The author would also like to acknowledge the use of the IRIDIS High Performance Computing Facility, and associated support services at the University of Southampton, in the completion of this work.

## CONFLICT OF INTEREST

The authors have declared no conflict of interest.

## DATA AVAILABILITY STATEMENT

The data that support the findings of this study are available from the corresponding author on reasonable request.

## ORCID

Peng Li  <https://orcid.org/0000-0003-1828-9597>

Jun-Yu Ou  <https://orcid.org/0000-0001-8028-6130>

## REFERENCES

1. Maher, M.-A., Nguyen, C.T., Stewart, H.D.: Vibrating Rf mems overview: Applications to wireless communications. *PROC SOC PHOTO-OPT INS* 5715, 11–25 (2005)
2. Bao, M., Yang, H., Sun, Y., et al: Modified Reynolds' equation and analytical analysis of squeeze-film air damping of perforated structures. *J. Micromech. Microeng* 13(6), 795 (2003)
3. Wenjing, Y., Xin, W., Hemmert, W., et al.: Air damping in laterally oscillating microresonators: A numerical and experimental study. *J. Microelectromech. Syst.* 12(5), 557–566 (2003)
4. Abdolvand, R., Johari, H., Ho, G.K., et al.: Quality factor in trench-refilled polysilicon beam resonators. *J. Microelectromech. Syst.* 15(3), 471–478 (2006)
5. Duwel, A.G.J., Weinstein, M., Borenstein, J., Ward, P.: Experimental study of thermoelastic damping in MEMS gyros. *Sensors Actuators A: Phys.* 103, 70–75 (2003)
6. Houston, B.H., Photiadis, D.M., Marcus, M.H., et al.: Thermoelastic loss in microscale oscillators. *Appl. Phys. Lett.* 80(7), 1300–1302 (2002)
7. Candler RN, L.H.: Investigation of energy loss mechanisms in micromechanical resonators. *Transducers '03, The 12th International Conference on Solid-State Sensors, Actuators and Microsystems: Digest of Technical Papers*, Boston, USA, June 2003, pp. 332–335
8. Astley, R.J.: Infinite elements for wave problems: A review of current formulations and an assessment of accuracy. *Int. J. Numer. Meth. Engng* 49, 951–976 (2000)
9. Cecil, Z.O., Taylor, R.L.: *The Finite Element Method: Solid Mechanics*, vol. 2. Butterworth-Heinemann, Oxford (2000)
10. Engquist, B., M.A.: Absorbing boundary conditions for numerical simulation of waves. *Proc. Natl. Acad. Sci.* 74(5), 1765–1766 (1977)
11. Givoli, D.: *Numerical methods for problems in infinite domains*. Elsevier, Amsterdam (2013)
12. Berenger, J.P.: A perfectly matched layer for the absorption of electromagnetic waves. *J. Comput. Phys.* 114(2), 185–200 (1994)
13. Steeneken, P.G., Ruigrok, J.J.M., Kang, S., et al.: Parameter extraction and support-loss in MEMS resonators. Preprint, arXiv:1304.7953 (2013)
14. Basu, U., Chopra, A.K.: Perfectly matched layers for time-harmonic elastodynamics of unbounded domains: Theory and finite-element implementation. *Comput. Methods Appl. Mech. Engng* 192(11–12), 1337–1375 (2003)
15. Bindel, D.S., Govindjee, S.: Elastic pmls for resonator anchor loss simulation. *Int. J. Numer. Meth. Eng.* 64(6), 789–818 (2005)
16. Thakar, V., R.-Z.M.: Optimization of tether geometry to achieve low anchor loss in Lamé-Mode resonators. *Joint UFFC, EFTF and PFM Symposium* 129–132 (2013)
17. Shahraini, S., Shahmohammadi, M., Fatemi, H., et al.: Side-supported radial-mode thin-film piezoelectric-on-silicon disk resonators. *IEEE Trans. Ultrason. Eng.* 66(4), 727–736 (2019)
18. Gerrard, D.D., Eldwin, J., Ng: Modeling the effect of anchor geometry on the quality factor of bulk mode resonators. *18th International Conference on Solid-State Sensors, Actuators and Microsystems*, pp. 1997–2000, Anchorage, AK. (2015)
19. Chen, Y.-Y., Yen-Ting, L.: Finite element analysis of anchor loss in aln lamb wave resonators. *International Frequency Control Symposium (FCS)*, pp. 1–5, Taipei, Taiwan, (2014)
20. Darvishian, A., Shiari, B., Cho, J.Y., et al.: Anchor loss in hemispherical shell resonators. *J. Microelectromech. Syst.* 26(1), 51–66 (2017)
21. Rodriguez, J., Chandorkar, S.A., Glaze, G.M., et al.: Direct detection of anchor damping in mems tuning fork resonators. *J. Microelectromech. Syst.* 27(5), 800–809 (2018)
22. Rodriguez, J., Chandorkar, S.A., Watson, C.A., et al.: Direct detection of akhiezer damping in a silicon mems resonator. *Sci. Rep.* 9(1), 2244 (2019)
23. Wu, G., Xu, J., Ng, E.J., et al.: Mem resonators for frequency reference and timing applications. *J. Microelectromech. Syst.* 29(5), 1137–1166 (2020)
24. Wang, Y., Lin, Y.-W., Glaze, J., et al.: Quantification of energy dissipation mechanisms in toroidal ring gyroscope. *J. Microelectromech. Syst.* 30(2), 193–202 (2021)
25. Hao, Z., Erbil, A., Ayazi, F.: An analytical model for support loss in micromachined beam resonators with in-plane flexural vibrations. *Sens. Actuators A* 109(1–2), 156–164 (2003)
26. COMSOL AB: *COMSOL multiphysics reference manual*. version 5.6. 387–396 (2020)
27. Johnson, S.G.: Notes on perfectly matched layers (PMLs). Preprint arXiv:2108.05348 (2021)

28. Frangi, A., Bugada, A., Martello, M., et al.: Validation of pml-based models for the evaluation of anchor dissipation in mems resonators. *Eur. J. Mech. A Solids* 37, 256–265 (2013)
29. Van Laer, R., Kuyken, B., Van Thourhout, D., et al.: Interaction between light and highly confined hypersound in a silicon photonic nanowire. *Nat. Photonics* 9(3), 199–203 (2015)
30. Erlandsson, S.: Evaluation, adaption and implementations of perfectly matched layers in comsol multiphysics. PhD Thesis, KTH Royal Institute of Technology, (2020)
31. Mercadé, L., Korovin, A.V., Pennec, Y., et al.: Vertical engineering for large Brillouin gain in unreleased silicon-based waveguides. *Phys. Rev. Appl.* 15(3), (2021)
32. Free Vibration of a Cantilever Beam (Continuous System). <http://vlab.amrita.edu/?sub=3&brch=175&sim=1080&cnt=1>. Accessed 16 Nov 2021
33. Jimbo, Y., Itao, K.: Energy loss of a cantilever vibrator. *J. HIJ* 47(1), (1968)
34. Photiadis, D.M., Judge, J.A.: Attachment losses of high Q oscillators. *Appl. Phys. Lett.* 85(3), 482–484 (2004)
35. Judge, J.A., Photiadis, D.M., Vignola, J.F., et al.: Attachment loss of micromechanical and nanomechanical resonators in the limits of thick and thin support structures. *J. Appl. Phys.* 101(1), (2007)
36. Darvishian, A., Shiari, B.: Effect of Substrate Thickness on Quality Factor of Mechanical Resonators. *IEEE ISISS Proc*, pp. 1–4, Hapuna Beach, HI, (2015)
37. Chen, S., Liu, J., Guo, F.: Evaluation of support loss in micro-beam resonators: A revisit. *J. Sound Vib.* 411, 148–164 (2017)
38. Chen, S., Yang, W., Song, J., et al.: A new mechanism of energy dissipation in nanomechanical resonators due to the Casimir force. *J. Appl. Phys.* 126(4), 044502 (2019)
39. Fung, Y.C., Tong, P., Chen, X.: *Classical and Computational Solid Mechanics*. World Scientific Publishing Company, Singapore (2017)

## SUPPORTING INFORMATION

Additional supporting information can be found online in the Supporting Information section at the end of this article.

**How to cite this article:** Li, P., Ou, J.-Y., Yan, J.: Method for optimising the performance of PML in anchor-loss limited model via COMSOL. *IET Sci. Meas. Technol.* 1–10 (2022).  
<https://doi.org/10.1049/smt2.12107>